Environment International 101 (2017) 59–69

Contents lists available at ScienceDirect

Environment International

journal homepage: www.elsevier.com/locate/envint

Full length article

ELF exposure from mobile and cordless phones for the epidemiological MOBI-Kids study

Carolina Calderón [a,*], Hiroki Ichikawa [b], Masao Taki [b], Kanako Wake [c], Darren Addison [a], Terry Mee [a], Myron Maslanyj [a], Hans Kromhout [d], Ae-Kyoung Lee [e], Malcolm R Sim [f], Joe Wiart [g], Elisabeth Cardis [h,i,j]

[a] Public Health England, Centre for Radiation, Chemical and Environmental Hazards, Chilton, Didcot, Oxon OX11 0RQ, UK
[b] Department of Electrical Engineering, Graduate School of Engineering, Tokyo Metropolitan University, Japan
[c] EMC Group, Applied Electromagnetic Research Center, National Institute of Information and Communications Technology, Tokyo, Japan
[d] Institute for Risk Assessment Science, Utrecht University, PO Box 80178, NL 3508 TD, Utrecht, The Netherlands
[e] Radio Technology Research Department, Electronics and Telecommunications Research Institute (ETRI), Yuseong-gu, Daejeon, Republic of Korea
[f] Department of Epidemiology and Preventive Medicine, Faculty of Medicine, Nursing and Health Science, Monash University, Alfred Centre, Commercial Road, Melbourne, Victoria 3004, Australia
[g] Télécom ParisTech, 37-39 Rue Dareau, 75013 Paris, France
[h] Barcelona Institute for Global Health (ISGlobal), Barcelona, Spain
[i] Universitat Pompeu Fabra (UPF), Barcelona, Spain
[j] CIBER Epidemiología y Salud Pública (CIBERESP), Madrid, Spain

ARTICLE INFO

Article history:
Received 26 August 2016
Received in revised form 6 January 2017
Accepted 6 January 2017
Available online 24 January 2017

Keywords:
EMF
ELF
Mobile phones
Induced current density
Magnetic fields
Epidemiology

ABSTRACT

This paper describes measurements and computational modelling carried out in the MOBI-Kids case-control study to assess the extremely low frequency (ELF) exposure of the brain from use of mobile and cordless phones. Four different communication systems were investigated: Global System for Mobile (GSM), Universal Mobile Telecommunications System (UMTS), Digital Enhanced Cordless Telecommunications (DECT) and Wi-Fi Voice over Internet Protocol (VoIP). The magnetic fields produced by the phones during transmission were measured under controlled laboratory conditions, and an equivalent loop was fitted to the data to produce three-dimensional extrapolations of the field. Computational modelling was then used to calculate the induced current density and electric field strength in the brain resulting from exposure to these magnetic fields. Human voxel phantoms of four different ages were used: 8, 11, 14 and adult. The results indicate that the current densities induced in the brain during DECT calls are likely to be an order of magnitude lower than those generated during GSM calls but over twice that during UMTS calls. The average current density during Wi-Fi VoIP calls was found to be lower than for UMTS by 30%, but the variability across the samples investigated was high. Spectral contributions were important to consider in relation to current density, particularly for DECT phones. This study suggests that the spatial distribution of the ELF induced current densities in brain tissues is determined by the physical characteristics of the phone (in particular battery position) while the amplitude is mainly dependent on communication system, thus providing a feasible basis for assessing ELF exposure in the epidemiological study. The number of phantoms was not large enough to provide definitive evidence of an increase of induced current density with age, but the data that are available suggest that, if present, the effect is likely to be very small.
© 2017 Elsevier Ltd. All rights reserved.

1. Introduction

The potential carcinogenic effects of electromagnetic fields (EMFs) from mobile phones have been extensively investigated (Benson et al., 2013; Cardis et al., 2011a, 2011b; Coureau et al., 2014; Frei et al., 2011; Hardell and Carlberg, 2015; Hardell et al., 2013; IARC, 2011; INTERPHONE Study Group, 2011; Swerdlow et al., 2011; The INTERPHONE Study Group, 2010). However, the studies completed so far have tended to focus on Radio Frequency (RF) EMF exposure in adults, without considering the extremely-low frequency (ELF) exposure produced by currents in the phones or whether children's brains are more susceptible to the hand-held phone exposures in general. MOBI-Kids is a

Abbreviations: 2G/3G, Second generation/Third generation; APC, Adaptive Power Control; CDMA, Code Division Multiple Access; CNS, central nervous system; CSF, cerebrospinal fluid; DECT, Digital Enhanced Cordless Telecommunications; EIRP, equivalent isotropically radiated power; ELF, extremely low frequency; EMF, electromagnetic fields; GSM, Global System for Mobile; kbps, kilobits per second; PDC, Personal Digital Cellular; RF, Radio Frequency; SAR, Specific Energy Absorption Rate; SD, standard deviation; UMTS, Universal Mobile Telecommunications System; VoIP, Voice over Internet Protocol.

* Corresponding author at: Public Health England, Centre for Radiation, Chemical and Environmental Hazards, Chilton, Didcot, Oxfordshire OX11 0RQ, UK.
E-mail address: Carolina.Calderon@phe.gov.uk (C. Calderón).

http://dx.doi.org/10.1016/j.envint.2017.01.005
0160-4120/© 2017 Elsevier Ltd. All rights reserved.

multi-national case-control epidemiological study that aims to address these research gaps by investigating the potential carcinogenic effects of childhood and adolescent exposure to both RF and ELF EMFs arising from mobile telephones and associated technologies, specifically in terms of tumours of the central nervous system (CNS) (Sadetzki et al., 2014).

This paper describes the current densities and electric field strengths induced in the brain as a result of the ELF magnetic fields generated by mobile phones when used against the head during voice calls. In the absence of clear and consistent evidence of human ELF effects at normal environmental levels of exposure, there is no clear indication of the most appropriate physical quantity to be related to possible long term health effects. However, magnetic fields can induce forces on electrical charges inside the body, thus exposure can be considered in terms of induced current density, a quantity that depends on the strength and frequency of the magnetic field, and is associated with well-defined biological processes such as stimulation of the central and peripheral nervous system. For this reason, the main exposure metric for the MOBI-Kids study was chosen to be the induced current density integrated over time. The advantage of this metric is that it combines frequency, spatial and temporal characteristics of the magnetic fields (Roosli, 2014). In this paper, induced electric fields are also considered as a further possible metric when conducting epidemiological studies of human health effects and mobile phone use, as it may result in different exposure gradients in the brain. Four communication systems were considered, namely Global System for Mobile (GSM), Universal Mobile Telecommunications System (UMTS), Digital Enhanced Cordless Telecommunications (DECT) and Voice over Internet Protocol (VoIP). These systems were introduced in Europe between the early 1990s to early 2000s, although mobile phone VoIP applications have only become available since 2007 (BBC, 2007). All of these systems are still in use today. Numerical modelling was also performed for Code Division Multiple Access 2000 (CDMA2000) and Personal Digital Cellular (PDC) phones as part of the study but is not reported here.

The results will provide an insight into the main factors contributing to ELF exposure in the brain from handheld phones and whether these differ materially from those influencing RF exposure. These data are also being used in the construction of an algorithm for estimating the ELF dose in the brain at the location of the tumour for each case, and at the same location for matched controls in the MOBI-Kids study.

2. Materials and methods

The methods employed in this study were based on the known transmission characteristics of the communication systems, and previous literature as discussed below.

For example, ELF signals produced by GSM phones have been investigated previously (Calderón et al., 2014; Ilvonen and Sarvas, 2007; Ilvonen et al., 2005; Jokela et al., 2004). These studies reported 217 Hz magnetic field signals and associated harmonics that resulted from the transmission frame structure of GSM. Measurements performed previously as part of MOBI-Kids (Calderón et al., 2014), suggested that flip and slide phones may have different magnetic field distributions to those of bar phones, although whether this translated to different induced current density distributions in the brain remained to be investigated. The amplitudes of the signals were found to be only poorly correlated with manufacturer, shape, battery type, battery voltage, battery dimensions and even year of release. The data from this study were used for the calculation of induced current densities for GSM bar and flip/slide phones.

Conversely, literature on ELF signals produced by other types of communication systems is very limited. To date, there has only been one publication on ELF induced current densities from UMTS phones (Gosselin et al., 2013), which reported a 100 Hz magnetic field, and the authors are unaware of any induced current density investigations on DECT and VoIP systems. The lack of ELF publications on UMTS could be due to the fact that transmission is constant and therefore the magnetic fields are presumed to be mainly static and thus unable to induce currents inside the body. Also, UMTS uses Adaptive Power Control (APC) where the transmitted power of the handset is continually adjusted to minimise interference and power consumption, which combined with highly efficient power regulation (Persson et al., 2012), leads to very low typical power levels (<1 mW) and power consumption. GSM phones also use APC but are not as power efficient as UMTS. The relationship between magnetic flux density and antenna power level has been measured for GSM (Calderón et al., 2014) but to date no such information is available for UMTS.

DECT has a frame structure similar to GSM, but with a frame length of 10 ms and a duty factor of 1:24, which would result in a pulsed magnetic flux density of 100 Hz and harmonics. The maximum peak power in DECT phones is 250 mW, eight times lower than GSM (Schiller, 2003).

Unlike the communication systems mentioned above, VoIP transmits voice calls over the internet in random bursts, with a maximum equivalent isotropically radiated power (EIRP) of 100 mW over 2.4 GHz Wi-Fi (ETSI, 2012). Mobile phone VoIP applications allow calls to be made over data mobile network as well, but a usage charge is typically incurred in doing so, thus most VoIP calls are performed over Wi-Fi. In this paper only Wi-Fi VoIP calls (in the 2.4 GHz band) were investigated.

2.1. Measurement protocol

Following a protocol similar to the one reported previously for GSM (Calderón et al., 2014), magnetic field measurements on the front face plane of the phones (hereafter referred as two-dimensional measurements) were performed for samples of DECT (N = 8), UMTS (N = 8) and VoIP (N = 4) phones. All measurements were made in an anechoic chamber to isolate the RF element of the set-up. These measurements were used to determine hotspot position and amplitude (hotspot refers to the maxima in the two-dimensional maps).

The x-y plane was defined as the plane parallel to the front surface of the phone (with y being along the main axis of the phone) and z the direction perpendicular to the phone's front surface. The origin of each scan was defined as the centre of the front surface of the phone, and the grid spacing was 10 mm. Following the same GSM methodology (Calderón et al., 2014), the measurement distance was set to be as far away from the phone as possible to avoid unwanted systematic effects but close enough to be able to detect the magnetic fields. On the basis of preliminary scoping measurements, the distance was thus set to 25 mm for UMTS (and VoIP) and 20 mm for DECT. Induced current density maps were computed for one phone from each group, and then scaled to the average hotspot magnetic flux density of its respective group. As the scaling was relative to the phone used for the modelling, the difference in measurement distance was inconsequential (Supplement S1).

The measurements were performed with a shielded Bartington Mag03-MS1000 fluxgate magnetometer (Bartington Instruments, Witney, UK) (DC to 3 kHz) mounted on an in-house robotic scanner made out of low permittivity Perspex (RS Components, Corby, UK) (Calderón et al., 2014). A PerkinElmer Instruments 7625 DSP (1 mHz to 250 kHz) lock-in amplifier was used to lock onto the frequency of interest and reduce the noise floor to below 1 nT. The frequency chosen for the measurements for UMTS, DECT and VoIP[1] was 100 Hz, based on a preliminary assessment and published literature, where for DECT and UMTS this was attributed to the frame structure (Andersen and Pedersen, 1997; Gosselin et al., 2013).

The eight DECT phones sampled were all of different models and covered 4 different popular makes, released between 1999 and 2008 (average 2005), with one of the makes rebranded under a certain telecommunication company. All the phones had two AAA batteries (2.4 V), except for one that had three AAA (3.6 V) batteries and another that had two AA (2.4 V) batteries. To carry out the measurements, an internal call was made between two DECT handsets via the DECT base unit. The DECT

[1] For one of the mobile phones VoIP measurements were performed at 37 Hz instead of 100 Hz as the signal at 100 Hz was found to be close to noise floor and the dominant frequency was found to be at 37 Hz. The data were later scaled to 100 Hz using spectral data sampled at the hotspot.

base unit and second handset were placed inside the anechoic chamber, at least 1 m away from the probe and handset under investigation.

For the UMTS measurements, eight mobile phone models were measured (1 slide, 3 bar, 4 smart phones), of 7 different makes. All were released between the year 2007 and 2011 (average was 2010) and had 3.7 V batteries (7 Li-ion, 1 Li-Po). Of the 47 phone models used previously for the GSM measurements (Calderón et al., 2014), which were released between 1997 and 2008 (average was 2003), only a couple were UMTS enabled. A Rhode & Schwarz CMU200 universal radio communication tester (Rohde & Schwarz UK Ltd., Ancells Business Park, Fleet, UK) was used to emulate a UMTS call at 1 mW power level for the assessments.

VoIP measurements were made on four smartphones of three different makes. The phones differed for VoIP and UMTS, except for one model where it was possible to compare the UMTS and VoIP measurements on the same phone. An access point (Belkin N1 Vision Wireless router model F5D8 232-4), compatible with the Institute of Electrical and Electronics Engineers (IEEE) 802.11n standard operating in the 2.4 GHz band, was connected to a broadband internet connection and placed in the anechoic chamber. A popular VoIP application was installed on the mobile phone under test and then connected via Wi-Fi to the access point. A laptop placed outside the anechoic chamber was used to receive the VoIP call, connected via Ethernet to another broadband connection. No base station emulator was available that allowed the use of commercial VoIP applications, so communication could not be set to a fixed/chosen data rate. Subsequently, the use of package-sniffing software (Wireshark, Wireshark Foundation Inc., California, USA) showed that regardless of the signal quality the IEEE 802.11 g standard was always utilised with an average data rate of 85 kilobits per second (kbps) (range 75–120 kbps). This is in agreement with the recommended data rate of 100 kbps for voice calls for a popular VoIP application.[2] Measurements were performed with and without speech but no material difference was observed.

2.2. Detailed measurements to determine loop parameters

In order to calculate the induced current densities (or electric field strengths) in the head, it is necessary to have a three dimensional map of the magnetic field across the volume of the head. Previous work has shown that it is possible to predict the field using an equivalent circular loop model (Calderón et al., 2014; Jokela et al., 2004; Tuor et al., 2005), parametrised by its radius (a), current (i), and distance to the surface of the phone (z_{loop}). The loop pattern was also observed during the assessment of 47 GSM phones for the MOBI-Kids study (Calderón et al., 2014; Findlay, 2011; Findlay et al., 2012).

The loop parameters (a, i, z_{loop})were estimated by minimising the squared residuals of the loop model to a set of detailed measurements made on one phone from each group, using the function *fmincon* of the Matlab Optimization Toolbox. The detailed measurements were: B_z as a function of distance z at the location of the hotspot (where $B_x = 0$ and $B_y = 0$), B_z along x; B_x along x; and B_y along y, all latter three with the x or y line passing through the hotspot. The detailed measurements were done with a FW Bell Hall Effect sensor (Pacific Scientific OECO 4607 SE International Way Milwaukie, Oregon USA, DC – 400 Hz) connected to the lock-in amplifier (allowing measurements as close as 3 mm to the phone but with a floor noise of 40 nT) and with the Bartington Mag03-MS1000 fluxgate magnetometer. For GSM, the phone used for the detailed measurements was chosen based on how well its two-dimensional pattern correlated with other phones within its group (Calderón et al., 2014). For the other communication systems, where the magnetic flux density was considerably lower, the choice was based on the feasibility of being able to measure the magnetic field as a function of distance from the phone, visually taking into account how similar its pattern was compared to the rest of the samples. Because the magnetic flux density is proportional to the current of the loop, the final model effectively had its current scaled to represent average magnetic flux densities across the sample (Supplement S1). The final model for each communication system also utilised typical hotspot position.

2.3. Spectral measurements

The low frequency magnetic field signals from the various communication systems studied tend to have non-sinusoidal waveforms, composed of several frequency components. Spectral measurements were available for 8 GSM phones from previously performed work (Calderón et al., 2014) and here additional spectral measurements were reported for all UMTS and VoIP phones assessed and 3 of the DECT phones. The measurements were performed at the position of the hotspot using a Bartington Mag03-MS1000 fluxgate magnetometer connected to a Picoscope 3424 virtual oscilloscope (Pico Technology Ltd., James House, Colmworth Business Park, St Neots, Cambridgeshire, UK), providing a frequency range up to 3 kHz. Each measurement was averaged over 20 samples, with the background level subtracted. In the case of VoIP, spectral measurements were also performed on 3 phones using a different VoIP application to investigate the possible effect of other applications. The induced current density maps were scaled to take into account average spectral information using frequency scaling (Findlay et al., 2012; Gosselin et al., 2013). For more information on how this was performed, see supplement S1.

For UMTS, the spectral measurements were performed as a function of transmitted RF power level to determine whether values should be scaled to typical power levels. A base station emulator was used to increase the power level of the phone in steps while simultaneously measuring the RF electric field strength and ELF magnetic flux density. The RF electric field was measured with a Seibersdorf Precision Conical Dipole (PCD) 8250 broadband antenna (30 MHz to 3 GHz, Seibersdorf Labor GmbH, Austria) connected to an Agilent N9020A MXA signal analyser (20 Hz to 8.4 GHz, Keysight Technologies UK, Wokingham, Berkshire, UK).

2.4. Numerical modelling

Numerical modelling was performed for the phones tested here and the GSM phones reported previously (Calderón et al., 2014) to estimate the current densities and electric fields induced inside the brain. The calculations were performed using in-house software based on the impedance method (Orcutt and Gandhi, 1988). To advance on the INTERPHONE methodology (Cardis et al., 2011b) which used homogeneous phantoms, and to consider the effect of age, as study subjects are under 25, MOBI-Kids utilises four anatomically detailed voxel head models representing four different ages (8, 11, 14, and adult). These phantoms were constructed by Information Technologies in Society (IT'IS) using detailed anatomical information derived from MRI images (Christ et al., 2010). Tissue conductivities were assigned for the frequencies of interest using the IT'IS database (Hasgall et al., 2015). At ELF frequencies the conductivities are based on data from (Gabriel et al., 1996), specifically for the brain - 0.06 S/m for white matter, 0.09 S/m for grey matter and 0.11 S/m for cerebellum. For the remaining 5% of brain tissues where no data are available, Hasgall et al. assigned tissue substitutions based on function of organ and/or tissue composition.[3] Anisotropies resulting from different conductivities along and across fibres for white matter and cerebellum, which may vary by a factor of 10 (Gabriel et al., 2009), were not taken into account in the models and no age dependence was assumed for the conductivities of tissues as such information is only available above 300 kHz (Gabriel, 2005).

The Induced current densities (electric field strengths) were computed at a resolution of 2 mm^3 for the various phantoms and these were transferred onto a 1 cm^3 reference grid in a manner similar to that used for INTERPHONE (Cardis et al., 2011b); In any given 1 cm^3 cube, the

[2] https://support.skype.com/en/faq/FA1417/how-much-bandwidth-does-skype-need.

[3] Gray matter, hippocampus, thalamus with conductivity 0.09 S/m; white matter and Commissura (anterior and posterior) with conductivity 0.06 S/m; Cerebellum, midbrain, pons and medulla oblongata with conductivity 0.11 S/m; and hypophysis, hypothalamus and pineal body with conductivity 0.52 S/m.

induced current density assigned was the average value across all brain tissues voxels in that cube. Up to thirteen different brain tissues were considered in the averaging within each cube. This averaging process has two effects; firstly, it filters out any tissues which are not strictly brain tissue, such as the cerebrospinal fluid (CSF) which has a large conductivity compared to other CNS tissues. Secondly, it allows for uncertainties in tumour location as it is unlikely that the origin of the tumour can be determined to within an uncertainty of <5 mm, especially considering that this involves estimating the tumour location in the available phantoms from the subjects' diagnostic scan.

Although there may be morphological differences in the head as a function of age (which may have an effect), the size of the brain is believed to reach 95% of its final volume by the age of 6 (Giedd et al., 2006) thus brain size is not expected to change substantially over the age pertinent to (frequent) mobile phone use. Had all four phantoms used for the numerical modelling been from the same individual at different ages the number of 1 cm^3 cubes would have been the same for all heads. However, variations in brain size and head anatomy across the general population meant that the 1 cm^3 voxel brain maps did not overlap exactly across all four heads. This poses a problem when estimating lifetime dose, as for the particular cubes in question, data are needed across all relevant heads (since start of mobile phone use). To overcome this difficulty, cubes with no data (as a result of lack of overlap with other brains) were assigned the maximum value from the closest cubes with data, based on the methodology used in the RF part of the study (Wiart, 2016).

3. Results

3.1. Magnetic flux density measurements

Visual inspection of the two-dimensional patterns of the magnetic flux density components (B_x, B_y and B_z) suggest that the circular loop model was generally applicable for all phones investigated, although occasionally small secondary loops were observed (Appendices A and B). For UMTS, the equivalent source loop position was similar to that observed for GSM bar phones (Calderón et al., 2014), but around 2 cm lower down for DECT phones. The standard deviation of the loop positions for both GSM and DECT was around 1 cm but around 2 cm for UMTS.

As found previously for GSM phones (Calderón et al., 2014) where the main harmonics extended up to at least the 8th harmonic, spectral components were a feature of the signals. For DECT phones, the odd harmonics of 100 Hz tended to be smaller than the consecutive even harmonics (Fig. 1). For these two communication systems, the variation in harmonic contribution to the total induced current density was small across the sample investigated (SD < 14% for both), compared to the variation in amplitude at the fundamental frequency in the two-dimensional scans (SD ~47% for DECT and 68% for GSM).

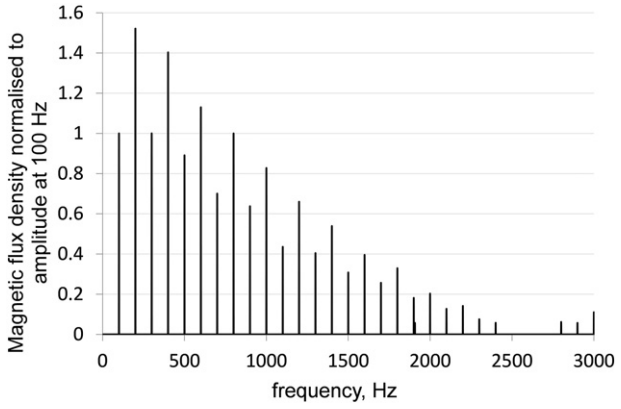

Fig. 1. Magnetic flux density spectrum for DECT phones normalised to the amplitude at 100 Hz. Spectrum measured with Mag03 at 20 mm from phone at the hotspot.

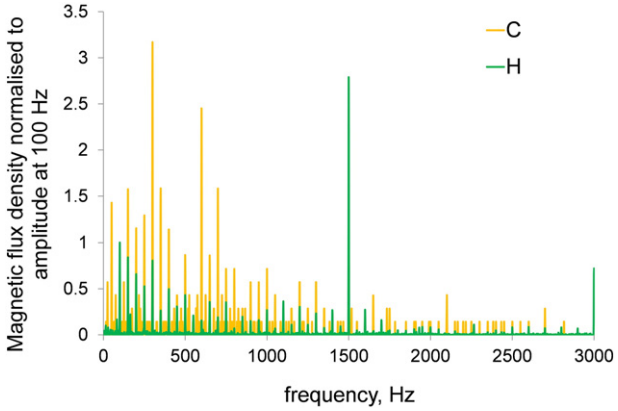

Fig. 2. Magnetic flux density spectrum normalised to the amplitude at 100 Hz for UMTS phones where the main spectral component was not 100 Hz (but 50 Hz harmonics were still present).

For UMTS, large spectral variations were observed across phones and 100 Hz was found to be the largest spectral component for only half of the phones assessed; the dominant spectral components for the remaining phones were 50 Hz, 200 Hz, 300 Hz and even 1.5 kHz (Fig. 2). Also, a 50 Hz harmonics signal was observed for the majority of phones, which was not due to the mains power supply of the probe as the signal was absent during background measurements.

For VoIP, the main spectral component varied across all phones although was always below 200 Hz. Most VoIP spectra showed a large number of small spectral components below 500 Hz (Fig. 3). Differences in spectrum were observed between the two popular VoIP applications investigated, and spectral contribution was found to be 1.3, 1.4 and 4.3 times larger for the second VoIP application. The spectra were measured for all VoIP and UMTS phones assessed because of the large variation.

Measurements using the base station emulator set at different power levels showed that AC magnetic flux density components were generally not dependent on power level during a UMTS call.

Two-dimensional measurements for the phone model that had both UMTS and VoIP capability showed the same hotspot position and the same decay with distance, with values overlapping when scaled to the amplitude of the hotspot at 25 mm. Their spectrums, however, differed considerably. It seems that only the amplitude (and spectrum) is likely to change depending on whether the call is made over VoIP or UMTS, and the magnetic field pattern remains largely unaffected. The overall magnetic field (including all spectral

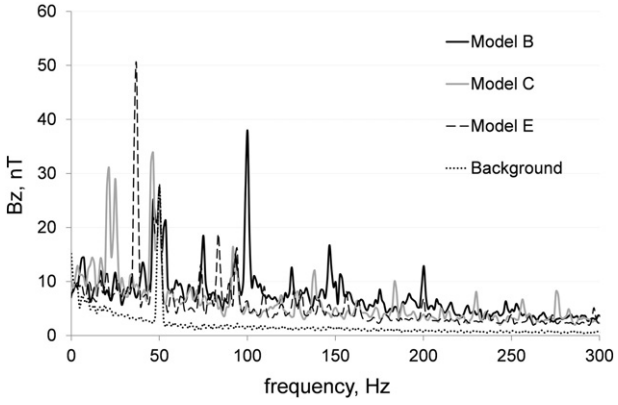

Fig. 3. Magnetic flux density spectrum for 3 phones measured during VoIP call. Measurement is the magnetic field component perpendicular to the phone, at the hotspot location. Not all spectra were included for clarity.

components) was found to be around 30% lower than that for UMTS. Based on these observations it was not considered necessary to undertake the numerical modelling for VoIP as induced current densities maps could be constructed using the UMTS maps scaled by a factor reflecting the amplitude (and spectrum) for VoIP, and likewise for induced electric fields.

3.2. Induced current density gradients and communication systems

The induced current density gradients for GSM (bar), GSM (flip/slide) and DECT suggest that the values are spread to the frontal contralateral side as the loop position shifts from the centre of the phone to the bottom of the phone (Fig. 4), particularly for the 8 year-old and the 11 year-old

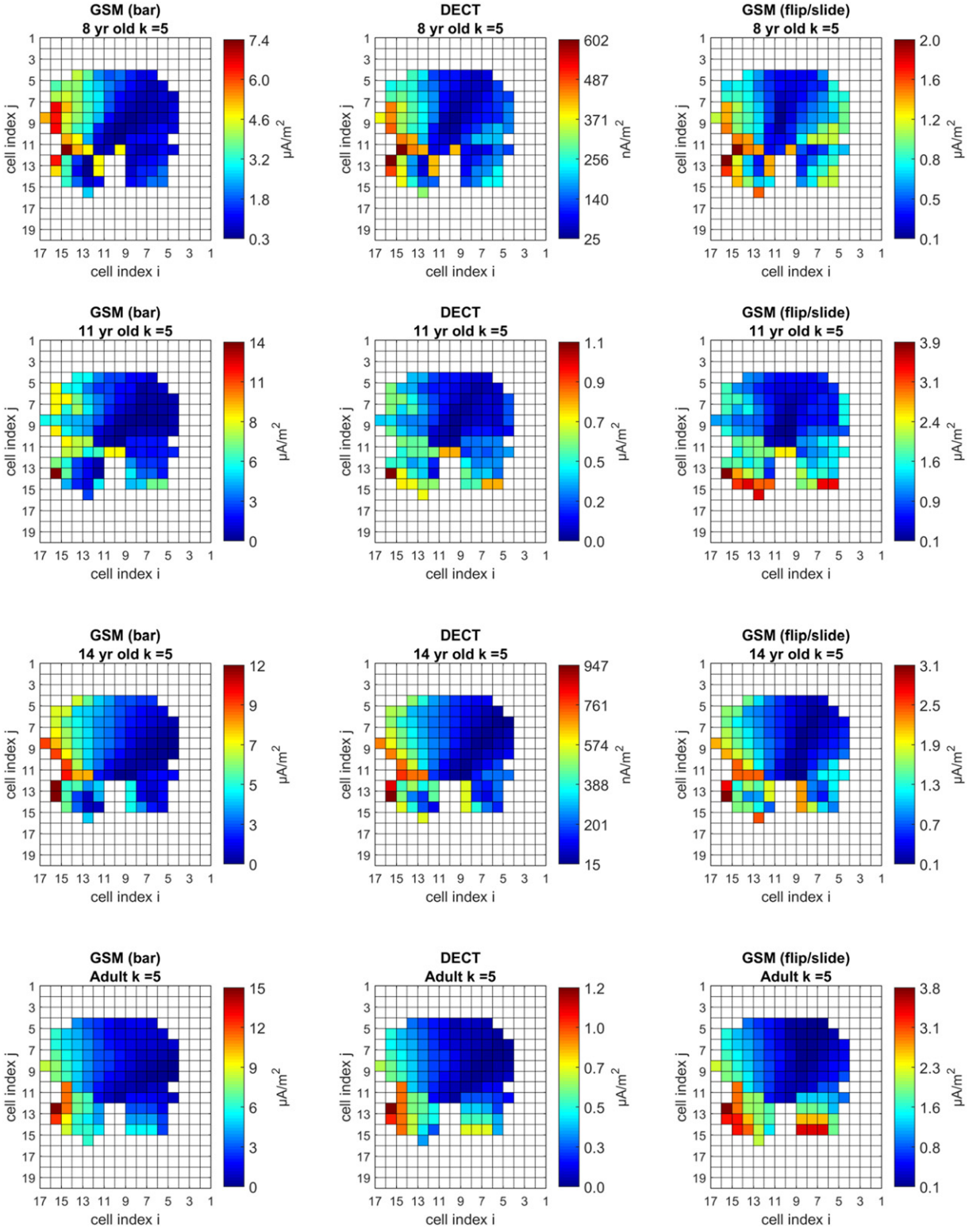

Fig. 4. Induced current density maps for the different heads (in plane k = 5) for GSM bar (left), DECT (centre) and GSM flip/slide (right). This is a top transverse/horizontal view of the brain, where index j increases from back to front of head, and i increases from left side of head to right side of the head. Maxima across all heads and communication systems were found either in plane k = 5 (half of the simulations) or on plane k = 6 or 7. Plane k = 5 is at the height of the ear. UMTS maps not shown as gradient was very similar to that of GSM bar (except 26 times lower in scale).

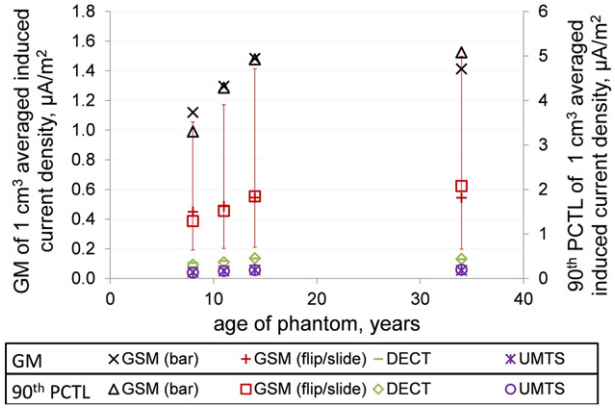

Fig. 5. Geometric mean (GM) and 90th percentile across all 1 cm^3 averaged induced current densities cubes as a function of age. GSD varied from 2.34 to 2.75. Error bars illustrate the location of one GSD in linear scale for GSM (flip/slide). The data on this graph are for the 1 cm^3 averaged maps before conversion to the 1 cm^3 reference brain grid, although results were very similar when using final maps.

heads. In the case of the 11 year-old brain, the maximum was actually found in the frontal left side (at k = 6, not shown), i.e. in the side opposite to where the phone is held, albeit within 1 cm to the left of the midline. The maxima were located typically at the height of the ear (Fig. 4).

The modelled induced current densities for UMTS and GSM bar phones showed strong similarities in gradient, with a Pearson correlation coefficient of over 0.99 for all four heads. The UMTS induced current density amplitudes were found to be around 25 times lower than GSM bar (where maximum

1 cm^3 induced current density was 15 $\mu A/m^2$), when accounting for spectral components. Slightly more pronounced differences were observed in the gradient for DECT, with GSM bar and DECT Pearson correlation coefficient of 0.92–0.93 across heads, and the maximum induced current density was found to be around 12 times lower than that observed for GSM bar phones. Due to APC, calls over GSM are typically transmitted at 50% maximum power level (Vrijheid et al., 2009). Because GSM measurements were performed with the phone transmitting at 1 W, the ratio between ELF induced current density from GSM versus that of DECT is 12 for GSM900 and 9 for GSM1800 when considering typical power levels (Calderón et al., 2014).

3.3. Induced current density versus age

Across the various phone systems investigated there is the suggestion of a slight increase in induced current density with age, as represented by the geometric mean and 90th percentile values (Fig. 5). The small increase, between 40% and 60% for both induced current densities and induced electric fields, had a non-parametric Spearman correlation equal to 1 for all except DECT (rho = 0.8), but the sample size was small (N = 4). Within this constraint, the non-monotonic variabilities observed in the induced current density distributions across the different heads suggest the differences are due to morphological variability across the population (and perhaps difference in head tilt across the different phantoms) and not age.

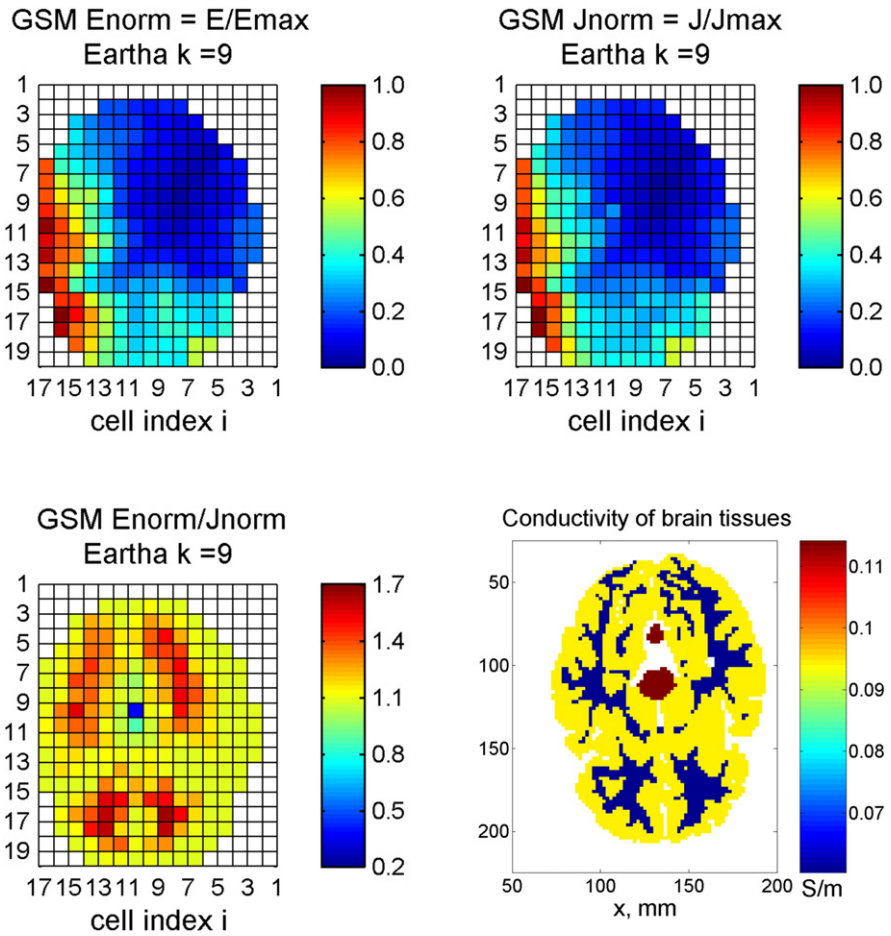

Fig. 6. Normalised induced electric field strength (top left) and normalised induced current density (top right) for the 1 cm^3 averaged cubes for GSM (bar) (k = 9), for Eartha (8 yr old). The bottom left plot highlights the differences between the two maps, and the one on the bottom right shows the conductivity of the tissues in a 2 mm plane in the centre of the k = 9 slice (not averaged over 1 cm^3).

3.4. Induced electric field versus induced current density gradients

For any given communication system and age, the induced current density and induced electric field strength gradients in the 1 cm^3 resolution maps were found to be very similar (Fig. 6). The small differences between the two maps become more apparent when plotting the ratio of the normalised maps, which revealed cubes of high and low conductivity (Fig. 6). A Pearson coefficient between 0.97 and 0.98 ($p < 1e\text{-}5$) was observed for the four heads when comparing the induced current density and induced electric field strength maps for the GSM bar phone. The average ratio between maximum induced electric field strength and maximum induced current density was 10.7 (V/m)/(A/m^2), with a range of 9.9–11.2 (V/m)/(A/m^2).

3.5. Uncertainties

The estimated uncertainty budget for the induced current density values is summarised in Table 1 where sources of uncertainty are listed and quantified based on the available information. It takes into account uncertainty due to measurement equipment (Table 1, item 1) and variation in magnetic flux density amplitude across the sample, from both two dimensional and spectral measurements (Table 1, item 2). The uncertainty estimates due to loop position, phone distance and representativeness of head models (items 3 to 5 respectively) are different across the 1 cm^3 cubes, and thus only mean values are provided. For example, uncertainty in distance between phone and head will result in larger induced current density uncertainty in cells closest to the phone. It should be noted that items 3 and 4 were approximations based on available data rather than based on additional numerical modelling. The uncertainty in tissue conductivities (item 6) is estimated from tissue inhomogeneity considerations (not anisotropy), and was set to 25 % based on work from (Gabriel et al. 1996).

4. Discussion

The investigation reported here was undertaken as part of a wider study to calculate the ELF induced current density integrated over time at the tumour location for case subjects (and the corresponding location for control subjects), and to ascertain the main determinants of the dose. Induced electric fields were also determined but, due to the relatively small variations in conductivities across brain tissues and the smoothing effect of the 1 cm^3 averaging, differences were subtle, suggesting both metrics would yield similar health risk outcomes.

The ELF induced current densities produced by GSM phones were found to be over an order of magnitude larger than those for UMTS. This means that in countries where these systems were used for voice calls, the ELF dose from mobile phones is likely to have decreased by $(95-\tau(t)\cdot 128)\%$ to $(96-\tau(t)\cdot 71)\%$ since the introduction of UMTS, where $\tau(t)$ is the proportion of voice calls transmitted over GSM at time t. The range arises from the possible relative proportions of GSM900 and GSM1800,[4] which have different typical power levels (i.e. for $\tau = 1$, where UMTS is not used, the range represents the relative induced current density amplitude between GSM900 and GSM1800; the lower range representing the prevalence changing from GSM1800 to GSM900 and vice versa for the higher range). That is, if presently GSM and UMTS are equally prevalent, then ELF dose has decreased between 31% to 60% in 15 years. The only published work on ELF exposure from UMTS (Gosselin et al., 2013) found exposure quotients (against ICNIRP 1998 basic restrictions) 70 times higher for GSM1800 in comparison to UMTS (SD ~ 20, N = 5), which is 2.7 times larger than the factor determined here. The disparity is probably due to a mixture of variability in the signal and differences in measurement and analysis protocol; their measurement was performed over a larger frequency range and closer to the source (thus more spectral components were included). They also included phase of the individual spectral components in their estimate, while this assessment uses a more conservative approach, summing the absolute value of the induced current density frequency components (Supplement S1). In any case, the results of (Gosselin et al., 2013) reinforce the implication that knowledge of the changing proportion of GSM and UMTS voice traffic over time will be important if accurate indices are to be obtained for the case and control subjects. Although GSM is beginning to be phased out in some countries, it is still the dominant communication system worldwide (Chambers, 2016). With regard to Wi-Fi VoIP, its low induced current density and low prevalence means it is likely to have a negligible contribution to the total ELF dose.

The relatively small variation in (normalised) spectra for GSM and DECT compared to UMTS and VoIP is expected to be due to the battery current waveform being dominated by the RF frame structure and the larger power used in the two former systems. The 100 Hz magnetic flux density signal observed in UMTS, which is independent of RF power level, could be due to tasks performed at every UMTS frame (10 ms), as suggested by Gosselin et al. (2013), or perhaps every speech frame (20 ms), which would also explain the 50 Hz component observed in most spectra. Similarly, even though the main frequency reported by Gosselin et al. was 100 Hz, their data also show harmonic components at 50 Hz (50 Hz itself was not observed as measurements started at 60 Hz). The 1.5 kHz signal observed in a few phones may be due to power control but related to processing rather than change in transmission power.

The maximum induced current density produced by cordless DECT phones was found to be much lower than that for GSM. This was expected, due to lower transmission powers (and thus lower currents) and the lower fundamental frequency in DECT. Also, the batteries in DECT phones are typically located lower in the handset than in GSM bar phones and are longer as well (hence the lower loop position observed), so the distance between the brain and the source is larger for DECT than for GSM bar phones. On the other hand, the contribution of harmonics to the total induced current density was found to be over 3 times higher in DECT phones. This is due to the harmonics extending to higher frequencies in DECT phones (due to the lower duty factor), and the fact that DECT current is drawn during reception as well as transmission (Andersen and Pedersen, 1997), resulting in the higher even harmonics observed in Fig. 1. All of this contributes to an estimated overall ratio of 12 between GSM and DECT maximum induced current density. However, because

Table 1
Uncertainty budget for the 1 cm^3 averaged induced current density values. All uncertainties are displayed as SD/AM (SD: standard deviation; AM: arithmetic mean). Average uncertainty across all cells is displayed where the sources of uncertainty is dependent on cell location.

Source	GSM (bar)	GSM (f/s)	DECT	UMTS	VoIP
Signal variation and instruments[a]	0.06	0.06	0.13	0.25	0.44
Loop current (and radius) in model (Variation in magnetic flux density across sample)[b]	0.69	0.60	0.49	0.66	0.88
Loop position along axis of phone[c]	0.14	0.14	0.14	0.28	0.28
Distance between phone and head[d]	0.37	0.37	0.37	0.37	0.37
Representativeness of head model[e]	0.3	0.3	0.3	0.3	0.3
Conductivity of tissues[f]	0.25	0.25	0.25	0.25	0.25
Total (k = 1)	0.89	0.82	0.75	0.93	1.15

[a] Taken from uncertainty budget for two-dimensional measurements.
[b] Combined standard deviation of the magnetic flux density two-dimensional measurements as well as spectral measurements.
[c] Based on normalised GSM and DECT maps such that the equivalent loop parameters were the same and only loop position along the phone axis differed. The calculation gave a mean uncertainty of <0.28 across all heads for a 2 cm uncertainty in loop position.
[d] Approximated by using the average uncertainty between 1 cm and 15 cm from the phone (brain position) in magnetic flux density along the axis of the loop due to an uncertainty in loop/phone distance to head of +/-1 cm.
[e] Based on the data from the 4 different heads used (assumes differences are only due to morphological differences and not age).
[f] (Gabriel et al., 1996) reported a variation in tissue conductivities at low frequencies of 15–25% due to inhomogeneity of tissues. Repeatability of measurements was 1%. Uncertainty due to anisotropy of tissues not included.

[4] The lower range corresponds to assuming only GSM1800 was used 15 years ago and presently GSM900 is used but GSM1800 is not, and vice versa for the higher range.

the lower loop position in DECT phones also led to slightly different induced current density distributions, the ratio can vary considerably across the brain. For example, looking at the induced current density in the 11 year old phantom (Fig. 4), the DECT phone induced current density is around a 25% of that of GSM in 3 cubes in the contralateral side (cubes (i = 4, j = 6–8)) when excluding typical power levels. Thus, although on average DECT induced current density is about an order of magnitude lower than GSM, the ratio will be dependent on tumour location.

Previous work conducted on GSM phones suggested that the type of phone, particularly the battery position, is likely to be an important determinant of the magnetic flux density hotspot (Calderón et al., 2014), and the same argument applies for the induced current density distribution inside the brain. The results of this and the previous study show that induced current density distributions are likely to be similar for GSM and UMTS phones. Also, some preliminary comparisons between UMTS and GSM patterns, made using four different phone models (not shown here), gave similar hotspot locations. These findings, together with the similarity in field patterns observed for UMTS and VoIP for the same phone suggests that, as expected, the induced current density distribution is dependent on the structure of the phone (e.g. battery position) rather than the communication system. Based on the above results, it is suggested that the GSM flip/slide maps be used for UMTS flip/slide phones, scaled by a factor of 26 to take into account the difference in amplitude and spectrum between the two communication systems. The fact that the induced current density distribution seems to spread to the frontal contralateral side as the equivalent loop position become lower in the phone is an interesting finding that sets it aside from the RF Specific Energy Absorption Rate (SAR) distribution. However, because of the variability in loop position across phones and variability in position of phone with respect to the head, this finding also highlights the uncertainty in induced current density distributions.

The results of this study, although based on a small sample size, suggest that age of the brain is unlikely to be a major factor in estimating induced current densities, and that morphological differences across the population are likely to be more important. Similarly, Gosselin et al. (2013) found no trend between surface-averaged current density and age, with variations across phones and uncertainty in loop position providing greater sources of variability. Likewise, in a study involving RF, the maximum SAR over 10 g was found to be effectively the same for children and adults because of the large inter-individual variability (Otto & von Muhlendahl, 2007; Wiart, Hadjem, Wong, & Bloch, 2008). Therefore, more focus on estimating the effect of variability in morphology across the population may be desirable.

The maximum 1 cm^3 induced current density for GSM (bar) was 15 $\mu A/m^2$ (before averaging, maximum 2 mm^3 induced current density was 235 $\mu A/m^2$ and found in the CSF). This value is relatively close to that reported by Ilvonen and Sarvas, (2007), where the 1 cm^2 maximum induced current density was 35 $\mu A/m^2$ in the central nervous system (CNS), excluding CSF. In comparison, the median residential magnetic flux density in the UK is 0.03 μT (N = 4969, (UKCCS, 2000)), which equates to 0.11 $\mu A/m^2$ maximum 1 cm^2 induced current density in the brain (excluding CSF), using data from Dimbylow which reports 3.56 $A/m^2/T$ in brain tissues for 50 Hz uniform fields (Dimbylow, 2008). In terms of time average induced current density, this is equivalent to less than 15 min/day of GSM900 voice call. However, for high residential exposures of 0.4 μT, this increases to 3 h/day. Thus heavy users of phones may be broadly equivalent to high exposures from traditional ELF sources.

In relation to household appliances held close to the head, Cheng et al. reported maximum induced current densities (with $(5\ mm)^3$ resolution phantoms) of 47 $\mu A/m^2$ and 3400 $\mu A/m^2$ from hair dryers (5 cm from head, N = 2) at 60 Hz (Cheng, Stuchly, DeWagter, & Martens, 1995), and Tofani et al. reported maximum induced current density (with $(13\ mm)^3$ resolution phantoms) of 10.9 $\mu A/m^2$ at 50 Hz (2 cm from head, N = 3) (Tofani, Anglesio, Ossola, & d'Amore, 1995). Both of these studies included CSF and thus could be up to 10 times larger than brain tissue induced current density. However, these values did not take into account the contribution of harmonics, thus are likely to underestimate the total induced current density. Maximum induced current densities of 87.6 $\mu A/m^2$ were also reported for razors (N = 6), and 16.9 $\mu A/m^2$ for drills (N = 3) for the dominant spectral component (Tofani et al., 1995). Apart from one of the hair dryers assessed by Cheng et al., all of these current densities are much lower than the endogenous levels in the body, which are reported to be of the order of 1 mA/m^2 (Cheng et al., 1995; NRC, 1997).

One of the main weaknesses of this investigation is it is based on a convenience sample, which may not be representative of the phones reported in the wider epidemiological study (whose distribution was not known a priori), or phones used in the wider population, and this may lead to sampling errors and bias. However, the sample of GSM phones was found to be a good representation of the proportion of market shares of the European mobile phone providers in the period of interest, with models released between 1997 and 2008 (Calderón et al., 2014) and collected from several participating countries. This same study found magnetic flux density amplitude was poorly correlated with different phone features and even year of release. Thus it is unlikely that changes in phone design over time would make a large difference in the ELF induced current densities calculated. The DECT, UMTS and VoIP samples were far smaller and therefore likely to be less representative, for example for DECT phones, where 3 of the 8 phones were rebranded under a certain telecommunication company. Thus the study could be improved in future by performing measurements on a larger and more representative sample of phones.

There are several sources of uncertainty in the results presented here, with implications for the generalisability of the data and on how well the induced current density maps reflect the contribution from each communication system. The method of assigning a given exposure to a group results in Berkson error, which reduces the power of the study (Gilbert, 2009). The largest contributor to uncertainty comes from the variation in magnetic flux density amplitude across the sample of phones (effectively the uncertainty in the current and radius of the loop model), which is of the order of 65% (k = 1) across the communication systems assessed. It should be noted that the spectral variability observed in UMTS is also present in the data of Gosselin et al. (2013), suggesting that this variability is an inherent feature in UMTS. Similar, if not larger, variations in magnetic flux density have been reported for household appliances in general; Preece et al. (1997) sampled 43 different types of appliances with over 10 samples each, resulting in an average SD/AM ratio of 1 at 5 cm from the appliances. Another source of uncertainty is in the distribution of the induced current densities. This is mostly attributable to variation in loop position across phone models, variation on the position of the phone with respect to the head, and morphological differences across the population. Lastly, there is a widely acknowledged lack of data on dielectric properties at low frequencies and on the possible variation as a function of age. The uncertainty in the dielectric properties in Table 1 comes from the inhomogeneity of tissues reported by Gabriel et al. (1996), although it is debatable whether this is likely to be a major source of uncertainty when averaging over 1 cm^3. The time-integrated ELF dose at the tumour location will have additional sources of uncertainty; namely uncertainties in the prevalence of GSM versus UMTS for voice calls as well as uncertainty in reported usage (number of calls, duration of calls, type of phone, and start and end usage dates) and tumour location. The uncertainty budget of the entire ELF algorithm used in the MOBI-Kids analyses will be described elsewhere.

5. Conclusion

This study investigated the current densities and electric field strengths induced in the brain as a result of the ELF magnetic fields generated by different types of handheld mobile phones used next to the head for voice calls.

Although the time variation of battery current and thus magnetic field will mimic that of the RF transmission (RF frame structure), the factors that affect RF exposure do not necessarily affect ELF exposure, or alter it differently. For example, ELF induced current density is proportional to

the frequency composition of the magnetic field waveform and thus, to a large extent, is dependent on RF frame structure. However, the latter only affects RF exposure when averaged over time (because of the duty factor). On the other hand, RF exposure is dependent on the carrier frequency of the communication system, while ELF exposure is not. Also, SAR is proportional to the transmitted power, while for ELF, the relationship has been shown to be less trivial. For instance, in the case of UMTS, the induced current density was found to be independent of power level.

The results suggest the overall amplitude of the induced current density is determined mainly by the communication system. The maximum 1 cm^3 averaged current density in the brain was found to be 15 $\mu A/m^2$, produced by GSM bar phones at a position in the brain at the approximate height of the ear. The current densities induced in the brain during DECT calls are likely to be an order of magnitude lower than those generated during GSM calls but over twice those during UMTS calls. Induced current density during Wi-Fi VoIP calls is likely to be approximately one third lower than for UMTS, although because of the small sample size, the variability in the measured values was high. VoIP calls are expected to contribute negligibly to the overall dose, especially when taking into account the low prevalence of use. Thus, for epidemiological purposes, knowledge of the changing proportion of GSM and UMTS voice traffic over time will be important if accurate exposure indices are to be obtained for the case and control subjects. The induced current density (and induced electric field) distributions were found to depend largely on the physical properties of the phone, with lower equivalent loop source positions resulting in a spread in values to the frontal contralateral side. Induced current density and electric field strength distributions in the brain were found to be very similar and if the induced current densities in the brain are affected by age, then the differences are likely to be very small.

The gradients reported here will be used together with usage and operator information from the wider MOBI-Kids study to estimate the ELF dose at the tumour location for the various case-control subjects. Thus, the factors most relevant to the ELF dose estimate and the effect of the various sources of uncertainty will need to be examined further.

Acknowledgements

The research leading to these results has received funding from by the European Community's Seventh Framework Programme (FP7/2007-2013) under grant agreement number 22687 3 – the MOBI-Kids project. We would like to thank Abdelhamid Hadjem for the helpful discussions on the averaging. We would also like to thank Sami Gabriel from Vodafone UK for the loan of some of the sample phones and the CMU200 emulator.

Appendix A. UMTS measurements results

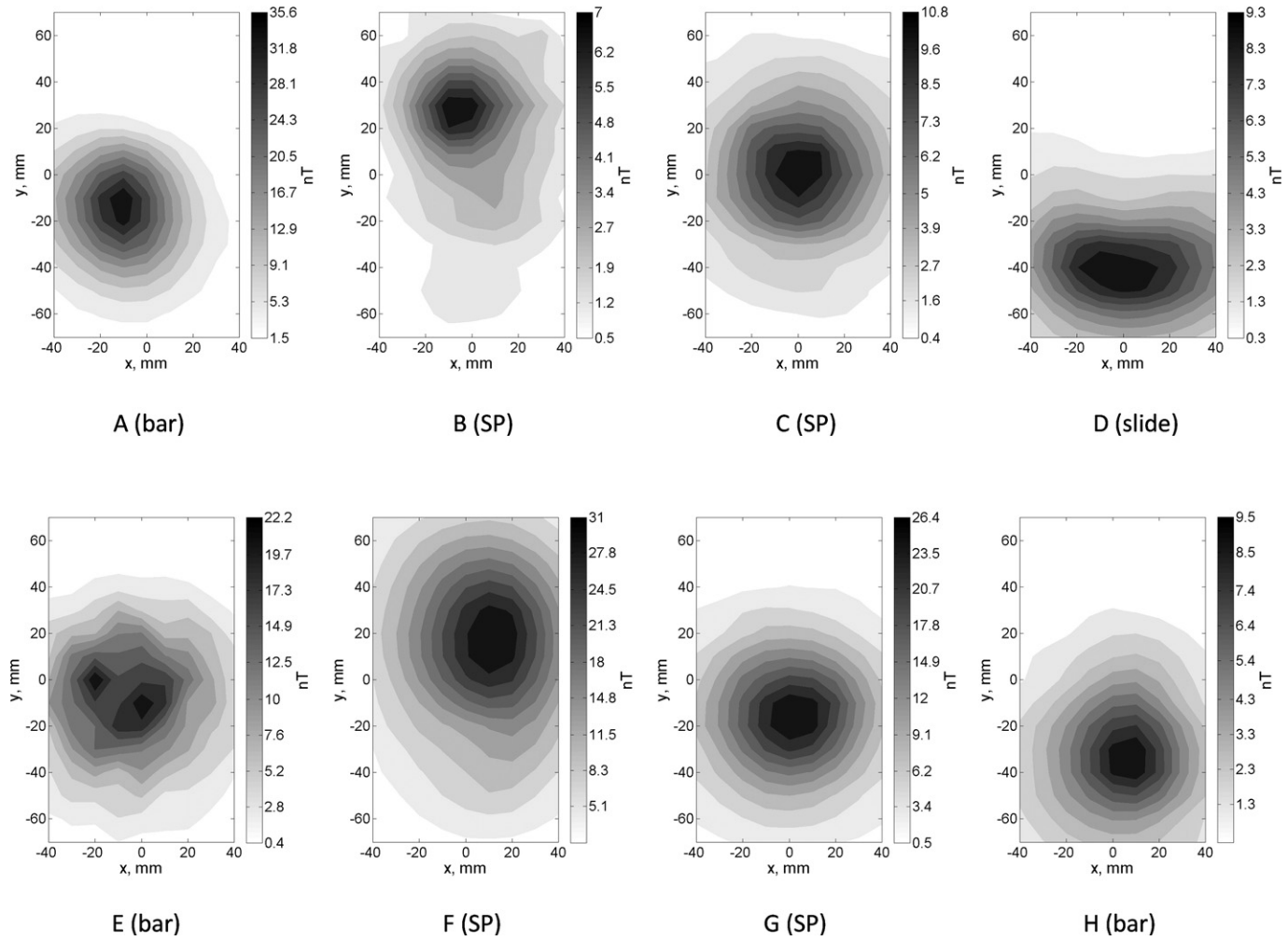

Fig. A1. Two-dimensional resultant maps at 100 Hz during UMTS voice call (measurements at 25 mm from phone). Power level used was 1 mW. Type of phone is shown in brackets (SP stands for smartphone).

Appendix B DECT measurements results

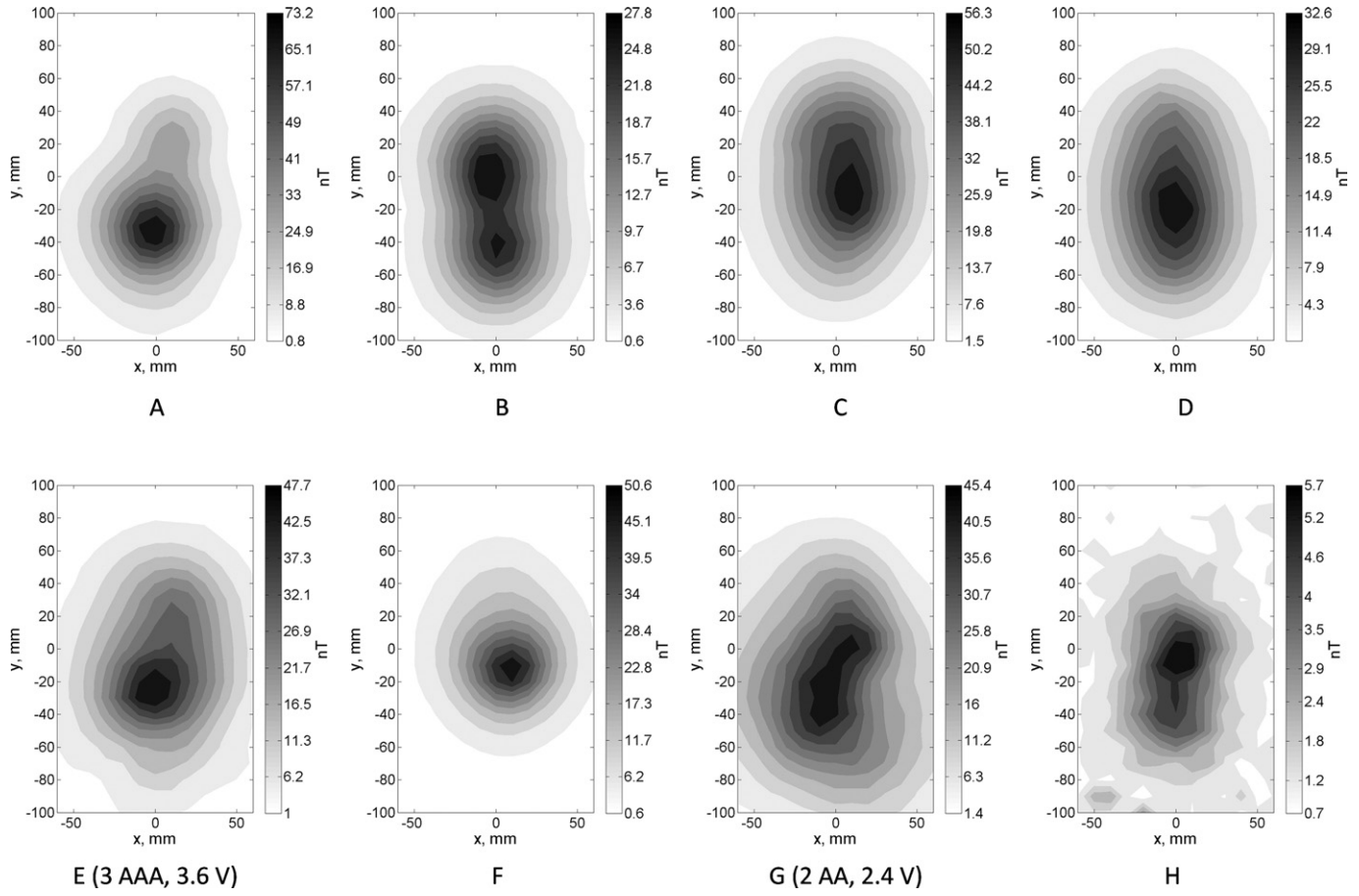

Fig. B1. Two-dimensional maps of resultant magnetic flux density at 100 Hz. All DECT phones had 2 AAA (2.4 V) batteries unless stated otherwise. Measurements at 20 mm from phone.

Appendix C. Supplementary data

Supplementary data to this article can be found online at http://dx.doi.org/10.1016/j.envint.2017.01.005.

References

Andersen, J.B., Pedersen, G.F., 1997. The technology of mobile telephone systems relevant for risk assessment. Radiat. Prot. Dosim. 72, 249–257.

BBC, 2007. Three Launches New SKYPE Mobile Phone. BBC (http://news.bbc.co.uk/1/hi/7066271.stm: BBC website).

Benson, V.S., Pirie, K., Schüz, J., Reeves, G.K., Beral, V., Green, J., Collaborators, f.t.M.W.S, 2013. Mobile phone use and risk of brain neoplasms and other cancers: prospective study. Int. J. Epidemiol.

Calderón, C., Addison, D., Mee, T., Findlay, R., Maslanyj, M., Conil, E., Kromhout, H., Lee, A.-K., Sim, M.R., Taki, M., Varsier, N., Wiart, J., Cardis, E., 2014. Assessment of extremely low frequency magnetic field exposure from GSM mobile phones. Bioelectromagnetics 35, 210–221.

Cardis, E., Armstrong, B.K., Bowman, J.D., Giles, G.G., Hours, M., Krewski, D., McBride, M., Parent, M.E., Sadetzki, S., Woodward, A., Brown, J., Chetrit, A., Figuerola, J., Hoffmann, C., Jarus-Hakak, A., Montestruq, L., Nadon, L., Richardson, L., Villegas, R., Vrijheid, M., 2011a. Risk of brain tumours in relation to estimated RF dose from mobile phones: results from five interphone countries. Occup. Environ. Med. 68, 631–640.

Cardis, E., Varsier, N., Bowman, J.D., Deltour, I., Figuerola, J., Mann, S., Moissonnier, M., Taki, M., Vecchia, P., Villegas, R., Vrijheid, M., Wake, K., Wiart, J., 2011b. Estimation of RF energy absorbed in the brain from mobile phones in the interphone study. Occup. Environ. Med. 68, 686–693.

Chambers, D., 2016. Mobile Network Statistics for 2016. Retrieved from. http://www.thinksmallcell.com/Opinion/mobile-network-statistics-for-2016.html.

Cheng, J., Stuchly, M.A., DeWagter, C., Martens, L., 1995. Magnetic field induced currents in a human head from use of portable appliances. Physics in medicine and biology 40, 495.

Christ, A., Kainz, W., Hahn, E.G., Honegger, K., Zefferer, M., Neufeld, E., Rascher, W., Janka, R., Bautz, W., Chen, J., Kiefer, B., Schmitt, P., Hollenbach, H.P., Shen, J., Oberle, M., Szczerba, D., Kam, A., Guag, J.W., Kuster, N., 2010. The virtual family–development of surface-based anatomical models of two adults and two children for dosimetric simulations. Phys. Med. Biol. 55, N23–N38.

Coureau, G., Bouvier, G., Lebailly, P., Fabbro-Peray, P., Gruber, A., Leffondre, K., Guillamo, J.S., Loiseau, H., Mathoulin-Pelissier, S., Salamon, R., Baldi, I., 2014. Mobile phone use and brain tumours in the CERENAT case-control study. Occup. Environ. Med. 71, 514–522.

Dimbylow, P., 2008. Quandaries in the application of the ICNIRP low frequency basic restriction on current density. Physics in medicine and biology 53, 133–145.

ETSI, 2012. EN 300 328 Electromagnetic Compatibility and Radio Spectrum Matters (ERM); Wideband Transmission Systems; Data Transmission Equipment Operating in the 2,4 GHz ISM Band and Using Wide Band Modulation Techniques; Harmonized EN Covering the Essential Requirements of Article 32 of the R&TTE Directive.

Findlay, R., 2011. D.P. Current Densities in a Voxel Model of the Head from Low Frequency Magnetic Fields Produced by a GSM Mobile Phone. In: society, T.B. (Eds.), 33rd Annual Meeting. Halifax, Canada.

Findlay, R.P., DPJ, Calderon, C., Maslanyj, M.P., 2012. Calculated Induced Electric Fields and Current Densities in Child Head Models From Exposure to Mobile Phones. 34th Bioelectromagnetics Annual Meeting. Brisbane, Australia.

Frei, P., Poulsen, A.H., Johansen, C., Olsen, J.H., Steding-Jessen, M., Schüz, J., 2011. Use of Mobile Phones and Risk of Brain Tumours: Update of Danish Cohort Study Ed^Eds.

Gabriel, C., 2005. Dielectric properties of biological tissue: variation with age. Bioelectromagnetics (Suppl. 7), S12–S18.

Gabriel, C., Peyman, A., Grant, E.H., 2009. Electrical conductivity of tissue at frequencies below 1 MHz. Phys. Med. Biol. 54, 4863.

Gabriel, S., Lau, R.W., Gabriel, C., 1996. The dielectric properties of biological tissues: II. Measurements in the frequency range 10 Hz to 20 GHz. Phys. Med. Biol. 41, 2251–2269.
Giedd, J.N., Clasen, L.S., Lenroot, R., Greenstein, D., Wallace, G.L., Ordaz, S., Molloy, E.A., Blumenthal, J.D., Tossell, J.W., Stayer, C., Samango-Sprouse, C.A., Shen, D., Davatzikos, C., Merke, D., Chrousos, G.P., 2006. Puberty-related influences on brain development. Molecular and cellular endocrinology 254-255, 154–162.
Gilbert, E.S., 2009. THE impact of dosimetry uncertainties on dose-response analyses. Health Phys. 97, 487–492.
Gosselin, M.C., Kuhn, S., Kuster, N., 2013. Experimental and numerical assessment of low-frequency current distributions from UMTS and GSM mobile phones. Phys. Med. Biol. 58, 8339–8357.
Hardell, L., Carlberg, M., 2015. Mobile phone and cordless phone use and the risk for glioma - analysis of pooled case-control studies in Sweden, 1997–2003 and 2007–2009. Pathophysiology 22, 1–13.
Hardell, L., Carlberg, M., Soderqvist, F., Mild, K.H., 2013. Case-control study of the association between malignant brain tumours diagnosed between 2007 and 2009 and mobile and cordless phone use. Int. J. Oncol. 43, 1833–1845.
Hasgall, P.A., DGF, Baumgartner, C., Neufeld, E., Gosselin, M.C., Payne, D., Klingenböck, A., Kuster, N., 2015. IT'IS Database for Thermal and Electromagnetic Parameters of Biological Tissues.
IARC, 2011. IARC Classifies Radiofrequency Electromagnetic Fields as Possibly Carcinogenic to Humans. (press release N° 208). WHO.
Ilvonen, S., Sarvas, J., 2007. Magnetic-field-induced ELF currents in a human body by the use of a GSM phone. IEEE Trans. Electromagn. Compat. 49, 294–301.
Ilvonen, S., Sihvonen, A.P., Karkkainen, K., Sarvas, J., 2005. Numerical assessment of induced ELF currents in the human head due to the battery current of a digital mobile phone. Bioelectromagnetics 26, 648–656.
INTERPHONE Study Group, 2011. Acoustic neuroma risk in relation to mobile telephone use: results of the INTERPHONE international case-control study. Cancer Epidemiol. 35, 453–464.
Jokela, K., Puranen, L., Sihvonen, A.P., 2004. Assessment of the magnetic field exposure due to the battery current of digital mobile phones. Health Phys. 86, 56–66.
NRC, 1997. Possible Health Effects of Exposure to Residential Electric And Magnetic Fields. ed^eds. National Academies Press.
Orcutt, N., Gandhi, O.P., 1988. A 3-D impedance method to calculate power deposition in biological bodies subjected to time varying magnetic fields. IEEE Trans. Biomed. Eng. 35, 577–583.
Otto, M., von Muhlendahl, K.E., 2007. Electromagnetic fields (EMF): do they play a role in children's environmental health (CEH)? International journal of hygiene and environmental health 210, 635–644.
Persson, T., Tornevik, C., Larsson, L.E., Loven, J., 2012. Output power distributions of terminals in a 3G mobile communication network. Bioelectromagnetics 33, 320–325.
Preece, A.W., Kaune, W., Grainger, P., Preece, S., Golding, J., 1997. Magnetic fields from domestic appliances in the UK. Phys. Med. Biol. 42, 67–76.
Roosli, M., 2014. Epidemiology of Electromagnetic Fields. (ed^eds). CRC Press.
Sadetzki, S., Langer, C.E., Bruchim, R., Kundi, M., Merletti, F., Vermeulen, R., Kromhout, H., Lee, A.K., Maslanyj, M., Sim, M.R., Taki, M., Wiart, J., Armstrong, B., Milne, E., Benke, G., Schattner, R., Hutter, H.P., Woehrer, A., Krewski, D., Mohipp, C., Momoli, F., Ritvo, P., Spinelli, J., Lacour, B., Delmas, D., Remen, T., Radon, K., Weinmann, T., Klostermann, S., Heinrich, S., Petridou, E., Bouka, E., Panagopoulou, P., Dikshit, R., Nagrani, R., Even-Nir, H., Chetrit, A., Maule, M., Migliore, E., Filippini, G., Miligi, L., Mattioli, S., Yamaguchi, N., Kojimahara, N., Ha, M., Choi, K.H., Mannetje, A., Eng, A., Woodward, A., Carretero, G., Alguacil, J., Aragones, N., Suare-Varela, M.M., Goedhart, G., Schouten-van Meeteren, A.A., Reedijk, A.A., Cardis, E., 2014. The MOBI-Kids study protocol: challenges in assessing childhood and adolescent exposure to electromagnetic fields from wireless telecommunication technologies and possible association with brain tumor risk. Front. Public Health 2, 124.
Schiller, J.H., 2003. Mobile Communications. (ed^eds). Addison-Wesley.
Swerdlow, A.J., Feychting, M., Green, A.C., Kheifets, L., Savitz, D.A., 2011. International commission for non-ionizing radiation protection standing committee on, e. mobile phones, brain tumors, and the interphone study: where are we now? Environ. Health Perspect. 119, 1534–1538.
The INTERPHONE Study Group, 2010. Brain tumour risk in relation to mobile telephone use: results of the INTERPHONE international case-control study. Int. J. Epidemiol. 39, 675–694.
Tofani, S., Anglesio, L., Ossola, P., d'Amore, G., 1995. Spectral analysis of magnetic fields from domestic appliances and corresponding induced current densities in an anatomically based model of the human head. Bioelectromagnetics 16, 356–364.
Tuor, M., Schuderer, E.S., Kuster, J., 2005. Assessment of ELF exposure from GSM handsets and development of an optimized RF/ELF exposure setup for studies of human volunteers. ITIS Foundation for Research on Information Technologies in Society.
UKCCS, 2000. The United Kingdom childhood cancer study: objectives, materials and methods. UK childhood cancer study investigators. Br. J. Cancer 82, 1073–1102.
Vrijheid, M., Mann, S., Vecchia, P., Wiart, J., Taki, M., Ardoino, L., Armstrong, B.K., Auvinen, A., Bédard, D., Berg-Beckhoff, G., Brown, J., Chetrit, A., Collatz-Christensen, H., Combalot, E., Cook, A., Deltour, I., Feychting, M., Giles, G.G., Hepworth, S.J., Hours, M., Iavarone, I., Johansen, C., Krewski, D., Kurttio, P., Lagorio, S., Lönn, S., McBride, M., Montestrucq, L., Parslow, R.C., Sadetzki, S., Schüz, J., Tynes, T., Woodward, A., Cardis, E., 2009. Determinants of mobile phone output power in a multinational study: implications for exposure assessment. Occupational and Environmental Medicine 66, 664–671.
Wiart, J., 2016. Personal Communication.
Wiart, J., Hadjem, A., Wong, M.F., Bloch, I., 2008. Analysis of RF exposure in the head tissues of children and adults. Physics in medicine and biology 53, 3681–3695.